JOURNAL OF THERMOPHYSICS AND HEAT TRANSFER
Vol. 13, No. 1, January–March 1999

Spectra and Critical Grashof Numbers for Turbulent Transition in a Thermal Plume

Katsuhisa Noto,* Kenji Teramoto,† and Tsuyoshi Nakajima†
Kobe University, Nada, Kobe 657-8501, Japan

Turbulent transition and turbulence characteristics of the thermal plume above a line heat source in unstratified air are elucidated by visualizing the plume, measuring the temperature, and analyzing the spectrum of the measured temperature. Large-scale vortices occur in the turbulent region, and they have the same frequency as the laminar swaying motion. Spectra S(s) can be approximated by $0.130f$ (Hz)$^{-5/3}$ in the inertia-convective subrange and $0.275f$ (Hz)$^{-3.0}$ in the inertia-diffusive subrange. The spectrum enables us to exactly determine the local state of flow, i.e., laminar, transitional, or turbulent. Grashof numbers for the beginning and end of a transition are $Gr_s = 2.0 \times 10^8$ and $Gr_e = 2.0 \times 10^9$. The transitional region is divided into the initial and final stages at $Gr_b = 7.52 \times 10^8$.

Nomenclature

f = frequency, Hz
$C(\tau)$ = autocorrelation function, K^2, $\overline{t(t_i)t(t_i + \tau)}$
d = diameter of heat source, mm
Gr_x = local Grashof number, $x^3 g\beta Q/\nu^2\lambda Pr$
g = gravitational acceleration, m/s^2
$h(0)$ = eigenvalue that is equal to 0.37326 for air
I = electric current, A
i = time-number of time-series data, or imaginary unit
L = length of heat source, mm
N = number of sampling data
$P(f)$ = power spectrum density, K^2 s, $\int C(\tau)\exp(-i2\pi f\tau)\, d\tau$
Pr = Prandtl number
$p(\eta)$ = probability density function, 1/K, $dProb[t(t_i) \leqq \eta]\, d\eta$
Q = convective heat rate per unit length of heat source, W/m, $Q_t - Q_r$
Q_r = radiative heat rate per unit length of heat source, W/m, $\varepsilon_m\sigma_s\pi d(T_w^4 - T_\infty^4)$
Q_t = heat rate generated per unit length of heat source, W/m, IV/L
$R(\tau)$ = autocorrelation coefficient, $C(\tau)/C(0)$
S = probability density function normalized by temperature variance, s, $P(f)/\sigma^2$
T = time-averaged temperature, K, $(\Sigma\, t_i)/N$
t = instantaneous temperature, K, $T + t'$
t' = temperature fluctuation, K, $t - T$
t_t = time, s
V = voltage difference between ends of heat source, V
x = vertical coordinate from heat source, mm
y = horizontal coordinate from heat source, mm
β = thermal coefficient of expansion, 1/K, $1/T_\infty$
δ = half-width of plume, mm
ε_m = emissivity of heat source
η = real quantity
θ = nondimensional temperature, $(T - T_\infty)/(T_{CL} - T_\infty)$
λ = heat conductivity, W/mK
ν = kinematic viscosity, m^2/s
ξ = nondimensional coordinate, $(y/x)Gr_x^{1/5}$
σ = standard deviation of temperature, K, $[\Sigma\, (t_i - T)^2/N]^{1/2}$
σ_s = Stefan–Boltzmann constant, W/m^{2}K^4
τ = time lag, s

Subscripts
b = at boundary between initial and final regions of transition
CL = on midplane
e = at end of transition
i = at i of time-series data
s = at beginning of transition
w = on heat source
∞ = far away from plume

Received Sept. 22, 1997; revision received July 27, 1998; accepted for publication Aug. 14, 1998.

*Department of Engineering. E-mail: noto@mech.kobe-u.ac.jp.
†Department of Engineering.

Introduction

LAMINAR thermal plume above a horizontal line heat source sways naturally from side to side without an artificial disturbance in both unstratified[1–5] and stably stratified[6–9] ambient. As a result, turbulent plume has two kinds of naturally time-dependent motions, i.e., one is the swaying motion and the other is turbulence, and is a very complicated time-dependent flow. The transitional and turbulent states of the plume in an unstratified ambient have been studied. First, Rouse et al.[10] and Lee and Emmons[11] analyzed the turbulent plume above the combusting heat source by the two-dimensional, steady boundary-layer theory. Rouse et al. measured only the time-averaged temperature on the midplane. Forstrom and Sparrow[1] measured the temperature and determined the critical Grashof numbers for the beginning and end of transition by the first appearance of turbulent bursts and a thickening of the plume width in the measured temperature on the given height. Bill and Gebhart[12] determined the critical Grashof numbers, which are larger than those by Forstrom and Sparrow, by the first signs of local turbulence in temperature time records and a thickening of the plume width by visualization. However, it is very difficult to find the first appearance of local turbulence with the swaying motion and to judge thickening of the plume width, because the former is extremely small in time records and the latter is based on macroscopically qualitative observation. Thus, time-averaged and dependent characteristics of the transitional and turbulent states in the plume have not yet been elucidated.

The beginning and end of transition are very important to clarify transitional and turbulent phenomena of the plume. The appropriate parameter for transition is the Grashof number. However, whether the downstream distance x, which is the additional parameter for transition[13–15] in buoyant flows along a vertical wall, is an additional parameter or not has not been made clear in the plume.

How can we determine accurately the critical Grashof number for transition from laminar to turbulent flow, and what is a character of turbulent transition in the plume? The purpose of the present study is therefore to obtain critical Grashof numbers and an additional parameter for transition by measuring time-dependent temperature and statistically analyzing the measured temperature, and to discuss transitional and turbulent phenomena in the plume that have not been made clear. The turbulent buoyant jet[16,17] is not referred to in this paper because it is governed by both momentum and buoyancy, and differs physically from the plume above a line heat source, which is governed only by buoyancy.

Experiment

Apparatus and Plume Generation

An experimental apparatus and measurement system are shown in Fig. 1. An enclosure with 800 × 800 mm^2 square cross section and 1000 mm height was used and was filled with air at atmospheric pressure. The temperature of the ceiling, bottom surface, and four side walls were isothermal. An electrically heated horizontal line heat source of a nichrome wire with d = 0.435 mm and L = 550 mm was placed at 400 mm above the bottom surface. Convective heat transfer rate, Q, from the wire is obtained by subtracting the radiative heat transfer rate, Q_r, from the heat generation rate, Q_h, and is in the range $8.73 \leqq Q$ W/m $\leqq 83.6$. In the present experiment, the heat source length L is longer than the 254 mm employed in previous experiments,[1,2] and the enclosure volume 0.64 m^3 is larger than 0.51 m^3 in Ref. 1 and 0.55 m^3 in Ref. 12. The aspect ratio L/d = 1264 is larger than 249 that was used in Ref. 1 and 741 in Ref. 12. The range of Q is wider than $1.77 \leqq Q$ W/m $\leqq 17.1$ in Ref. 1 and $13.0 \leqq Q$ W/m $\leqq 67.8$ in Ref. 12.

Plume Visualization and Temperature Measurement

The plume is visualized by the schlieren method. The plume velocity is not measured, but the plume temperature is measured because of the following.

1) The time-dependent velocity measured with a laser-Doppler velocimeter cannot give an accurate spectrum because a tracer does not move exactly with a turbulent flow.

2) Low velocity cannot be measured with a hot-wire velocimeter with temperature compensation.

3) Because the Prandtl number of air as plume fluid is around 0.7, which is slightly smaller than 1.0, flow and temperature visualizations showed that the plume flow is closely related to the plume temperature.

Thermocouples of 25.0–100.0 μm diameter with a fine constant larger than 25 Hz were employed and were sensitive and reasonable for the measurement of time-dependent temperature of the turbulent plume, because the dominant frequency of the plume temperature was less than 1.0 Hz. Physical properties were determined at the reference temperature T_r defined as $[T_{CL} - 0.38(T_{CL} - T_\infty)]$.

Acquisition of Time-Series Temperature and Statistical Analysis

The output from the thermocouple was input into an A/D board. The temperature was discretized by the A/D board and was stored on a floppy disk of a microcomputer. The time and number for sampling digitized temperature were determined by the method discussed by Noto and Matsumoto.[18] The Nyquist frequency in the present sampling process was much larger than the plume frequency. The temperature resolution was smaller than 0.1 K, which is sufficient for accuracy of statistical analysis. The present sampling is therefore reasonable for measurement, spectrum analysis, and discussion of transitional and turbulent states.

The time-averaged temperature and fluctuation intensity defined in the Nomenclature were obtained from the time-series temperature, which was analyzed statistically by using a microcomputer system; the autocorrelation coefficient (ACC), the probability density function (PDF), and the power spectrum density (PSD) were obtained by the maximum entropy method (MEM).[19,20]

Validity of Plume Formation, Measurement, and Statistical Analysis

By applying the plume light pl_1, pl_2, and pl_3 shown in Fig. 1, the plume motion was verified to be without the meandering motion[21] defined as the oscillation to the z direction, and with the swaying motion defined as the oscillatory motion in the x–y plane, and is two dimensional. The plume temperature of the laminar, transitional, and turbulent regions was also verified to be time-averaged two dimensional. The time-averaged temperature in the laminar region on the midplane was independent of time and agreed well with the previous re-

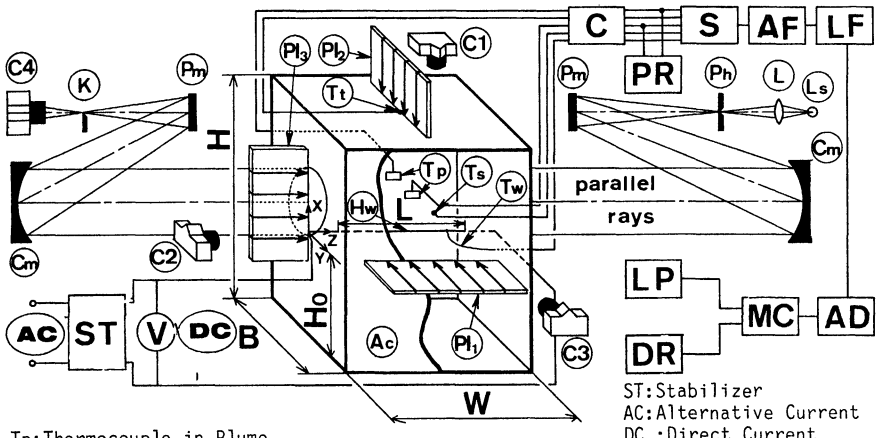

Fig. 1 Experimental apparatus and measurement system.

sults.[1,2,4,12,22,23] This means that the inevitable internal flow circulation in the test chamber did not affect the results. The laminar spectrum caused by the swaying motion had the gradient $-9/2$ and -8.0 in diagram of $\log S - \log f$, and agreed well with the expression by Noto.[4] The plume formation, measurement, and statistical analysis are therefore accurate and reasonable.

Measured Results

It was impossible to determine laminar, transitional, or turbulent region by observing the measured data shown in Figs. 2–8. The boundary between laminar and transitional regions, or transitional and turbulent regions determined in the next section and the boundary between initial and final transitional regions determined in this section are, therefore, plotted in every figure by using the following symbols: ▲ = laminar and transitional regions, △ = transitional and turbulent regions, and ↑ = initial and final transitional regions. The heating rates Q W/m = 8.73 and 27.8 ≦ Q W/m ≦ 83.6 are named *low rate* and *high rate*, respectively. Comparisons are made with previous results whenever possible.

Plume Visualization

Instantaneous visualizations of the plume are shown in Fig. 2, where the heated wire is at $(x, y) = (0, 0)$. Large-scale vortices are visible in the turbulent region, and have the same frequency as the swaying motion. However, the vortices were not visible in a Mach–Zehnder interferometer[12] because of the

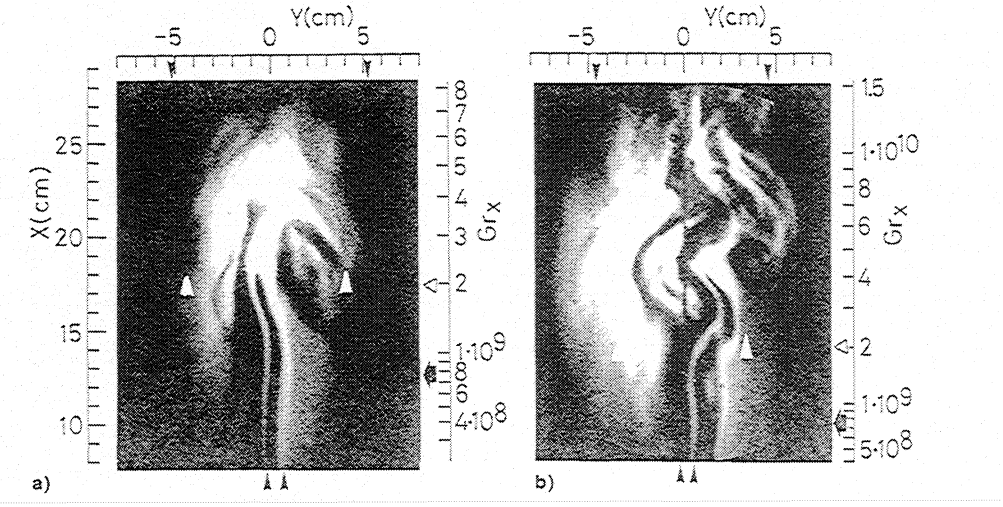

Fig. 2 Plume visualization. Q = a) 46.3 and b) 83.6 W/m.

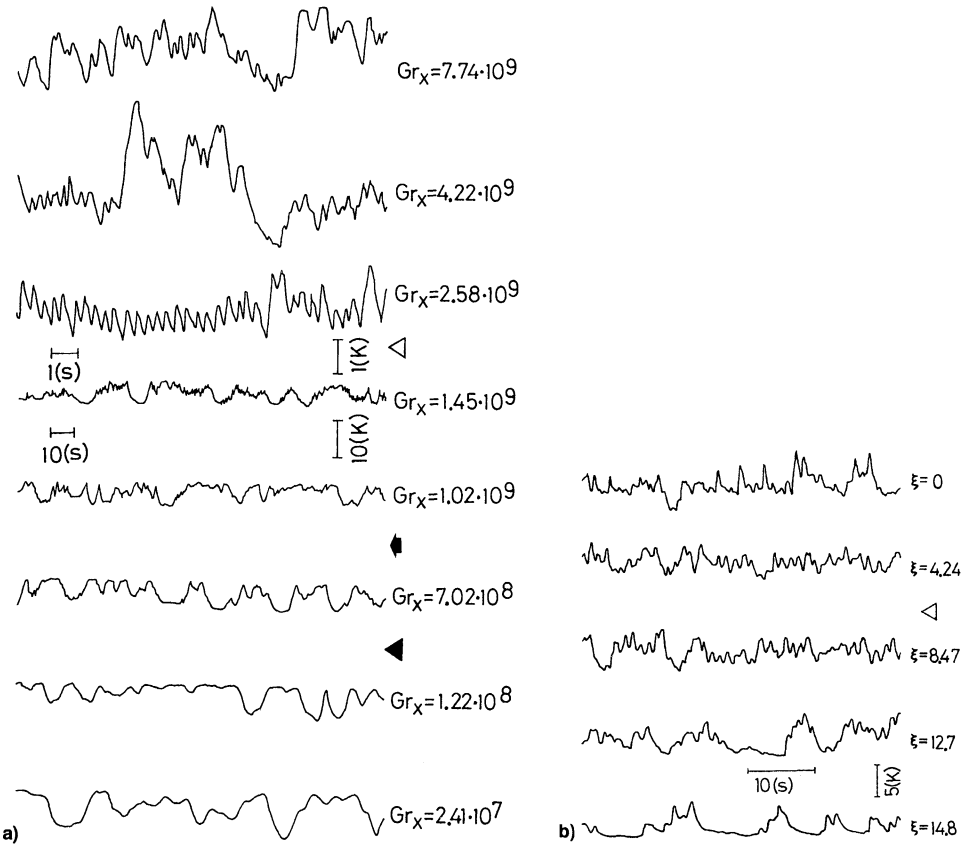

Fig. 3 Time record of temperature. On a) midplane at Q = 27.8 W/m and b) a given height at $Gr_x = 5.58 \times 10^9$ and Q = 83.6 W/m.

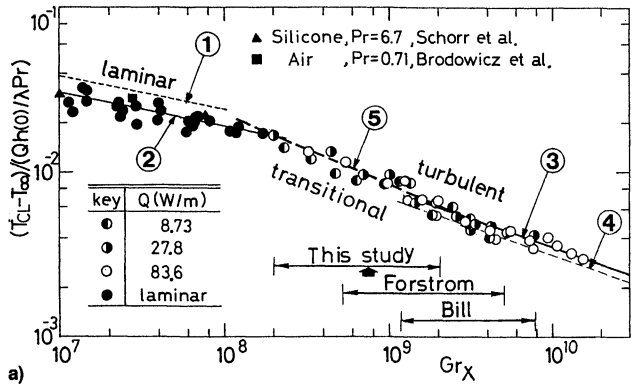

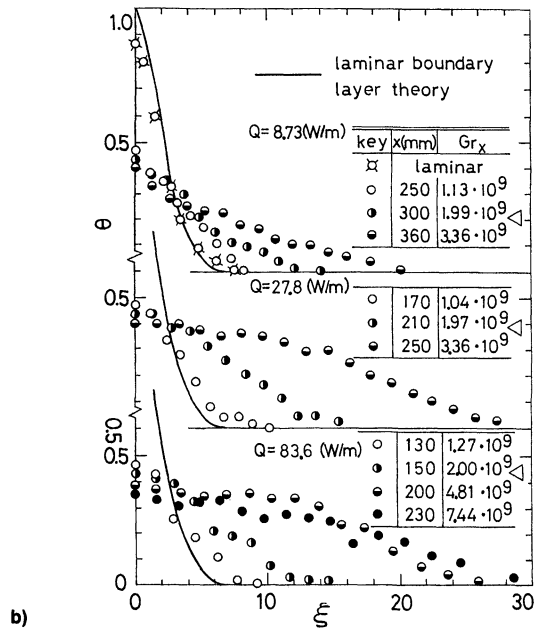

Fig. 4 Time-averaged temperature. On a) midplane and b) given height.

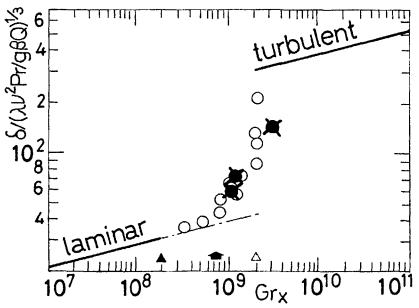

Fig. 5 Half-width of plume.

visualization of very small fluctuations of temperature. The plume half-width obtained by Eqs. (5) and (6) in the following section is shown by the black-colored arrows on the bottom and upper lines and by the white-colored arrows in Fig. 2. The plume thickens with increasing x because of turbulence, large-scaled vortices, and entrainment of air from the ambient. The plume in the transitional region inclines a little to the left and right directions in Figs. 2a and 2b, respectively, as a result of the swaying motion.

Temperature Time Record

Time records of temperature on the midplane are shown in Fig. 3a. Note that the scales of the time and temperature

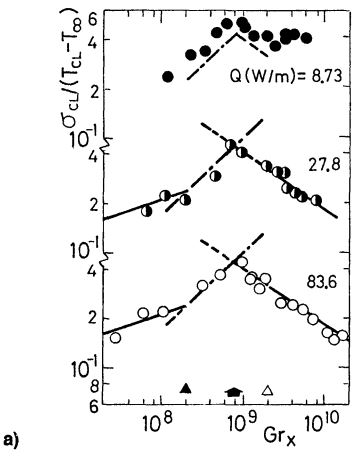

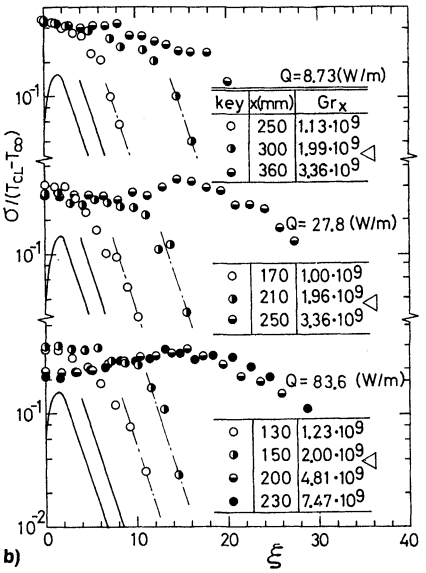

Fig. 6 Fluctuation intensity of temperature. On a) midplane and b) given height.

change at $Gr_x = 2 \times 10^9$. In the laminar region, the fluctuation is a result of only the swaying motion with the constant, maximum instantaneous temperature. In the transitional and turbulent regions, the fluctuation is affected by both the swaying motion and turbulence. The fluctuation with very small amplitude and period, which can be regarded as local turbulence, appears in the initial transitional region, develops in the final transitional region, and becomes dominant in the turbulent region.

Figure 3b shows time records on the given height with a turbulent state of $y = 0$ ($\xi = 0$). The region on and near the midplane is turbulent and the region far away from the midplane is transitional. Laminar-like fluctuations with the low temperature caused by the intermittent entrainment of ambient air into the plume appear in the transitional region far away from the midplane. This phenomena always occur at any heat rate.

Time-Averaged Temperature

Midplane

Figure 4a shows the time-averaged temperature on the midplane, where the horizontal lines show the transitional regions obtained by Forstrom and Sparrow,[1] Bill and Gebhart,[12] and the present study in the next section. Dotted line ① shows the temperature obtained by the laminar, steady boundary-layer theory.[24] Solid line ② is the laminar one measured in the present experiment. It agrees well with previous experiments[1,12]

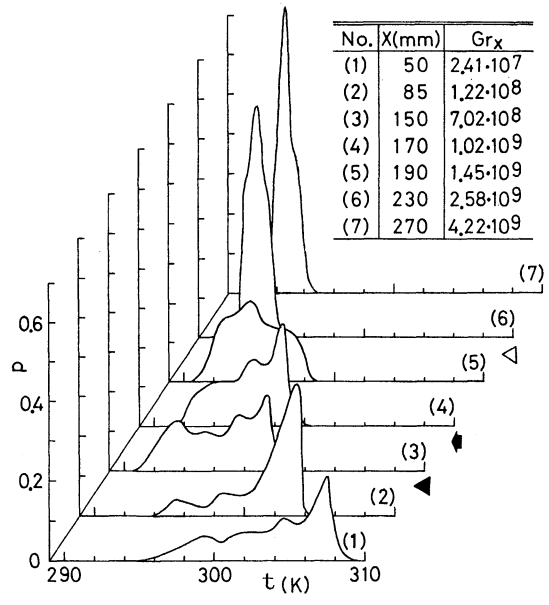

Fig. 7 PDF at Q = 27.8 W/m.

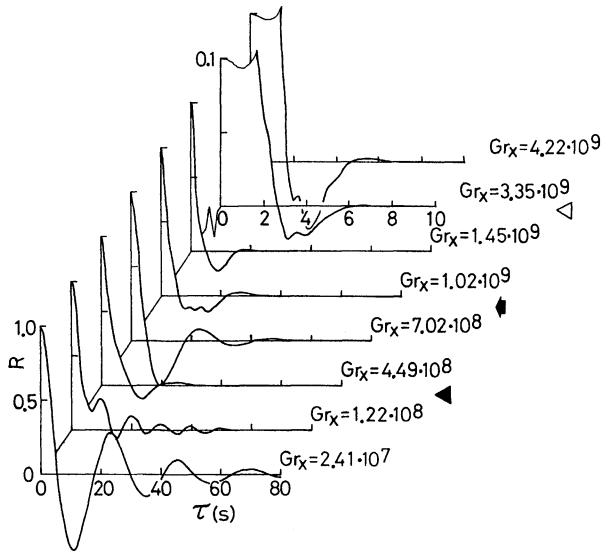

Fig. 8 ACC at Q = 27.8 W/m.

and is smaller by 15% than the laminar boundary-layer theory. It can be approximated as follows.

Laminar region:

$$(T_{CL} - T_\infty)/[Qh(0)/\lambda Pr] = 0.85Gr_x^{-1/5} \quad (1)$$

Solid line ③ is the result in the turbulent region determined by the present experiment as follows.

Turbulent region:

$$(T_{CL} - T_\infty)/[Qh(0)/\lambda Pr] = 7.52Gr_x^{-1/3} \quad (2)$$

where the temperature difference depends on $Q^{2/3}$ and agrees with Ref. 12. Dotted line ④ shows the result obtained by Rouse et al.[10] for the turbulent plume above the combusting heat source. It is expressed in a way similar to Eq. (2), but is smaller by 7.5% than that of Eq. (2).

Bold-dotted line ⑤ is the result in the transitional region determined by the present experiment as follows.

Transitional region:

$$(T_{CL} - T_\infty)/[Qh(0)/\lambda Pr] = 2.67 \times 10^2 Gr_x^{-1/2} \quad (3)$$

Table 1 m and n in $Q^m x^n$

	$T_{CL}-T_\infty$		δ		σ_{CL}	
Flow region	m	n	m	n	m	n
Laminar	4/5	−3/5	−1/5	2/5	29/30	−1/10
Initial transitional	1/2	−3/2	——	——	29/30	−1/10
Final transitional	1/2	−3/2	——	——	1/6	−5/2
Turbulent	2/3	−1	−1/5	2/5	1/3	−2

The value of $(T_{CL} - T_\infty)$ in the laminar, transitional, and turbulent regions is proportional to $Q^m x^n$, where m and n are shown in Table 1. The slope, i.e., $-n$, in the transitional region is larger than those in the laminar and turbulent regions because of the great increase of the half-width in the transitional region, as will be shown in Fig. 5.

Given Height

The measured temperature on the given height is shown in Fig. 4b with the laminar abscissa ξ and ordinate θ, where $T_{CL}[=T_\infty + Qh(0)Gr_x^{-1/5}/\lambda Pr]$ in θ is obtained by the laminar boundary-layer theory,[24] and laminar temperature was measured at $1.77 \leqq Q$ W/m $\leqq 17.1$ by Forstrom.[1] From Eqs. (1) and (2), the measured temperature at $y = 0$ is $\theta = 0.85$ and $\theta = 7.52Gr_x^{-2/15}$ in the laminar turbulent regions, and is smaller than the laminar theory value.[24] The temperature decreases and approaches the ambient temperature with increasing y.

The temperature in turbulent state at $y = 0$ at high Q rate was correlated[21] better by the abscissa ξ than y/x, and was approximated by the following relation, which can be transformed to the type of Rouse's equation when the cosine function is approximated by using the exponential one at $(\xi\pi/36) \ll 1.0$.

With turbulent at the midplane:

$$Gr_x^{1/3}(T - T_\infty)/(Q/\lambda Pr) = 2.81[1 + \cos(\xi\pi/36)]/2 \quad (4)$$

The turbulent temperature at the low Q rate was smaller than Eq. (4) at the high Q rate, approaching Eq. (4) with increasing Gr_x. The turbulent temperature at $8.73 \leqq Q$ W/m $\leqq 83.6$ therefore cannot be approximated by a single line.

Half-Width

The half-width of the plume is defined as the horizontal length between the midplane and the location at $T = (T_{CL} - T_\infty)/2$ in the time-averaged temperature on the given height. The laminar and turbulent halfwidths at the high Q rate are obtained from the experiment[4] and Eq. (4), respectively, as follows:

$$\delta/x = 2.50Gr_x^{-1/5} \quad (5)$$

$$\delta/x = 18.0Gr_x^{-1/5} \quad (6)$$

The half-widths normalized by a value without x are correlated as follows.

Laminar half-width:

$$\delta/(\lambda\nu^2 Pr/g\beta Q)^{1/3} = 2.50Gr_x^{2/15} \quad (7)$$

Turbulent half-width:

$$\delta/(\lambda\nu^2 Pr/g\beta Q)^{1/3} = 18.0Gr_x^{2/15} \quad (8)$$

The half-width is proportional to $Q^m x^n$, where m and n are shown in Table 1. The half-width in the laminar, transitional, and turbulent regions is shown in Fig. 5, where the solid lines represent Eqs. (7) and (8), and the white and black circles are the measured results in the transitional region at high and low rates, respectively. The half-width at the end of transition becomes 9.8 times as thick as that at the beginning of transition,

through a gradual increase in the initial transitional stage and a greater increase in the final one.

Fluctuation Intensity

Midplane

The fluctuation intensity normalized by $(T_{CL} - T_\infty)$ on the midplane is shown in Fig. 6a. Because characteristics at the high rate differed from that at the low rate, discussions are separated into the high and low rates, as follows.

At the high rate, the intensity in the turbulent region is approximated by Eq. (9), shown by the solid line on the right side in Fig. 6a. Equation (9) is transformed by employing Eq. (2), and the intensity is normalized by a value without x as follows.

Turbulent region:

$$\sigma_{CL}/(T_{CL} - T_\infty) = 400 Gr_x^{1/3} \tag{9}$$

$$\sigma_{CL}/(Q/\lambda Pr) = 1.12 \times 10^3 Gr_x^{-2/3} \tag{10}$$

The intensity in the final transitional stage is approximated by Eq. (11), shown by the dotted line in Fig. 6. Equation (12) is obtained from Eqs. (11) and (3) as follows.

Final transitional region:

$$\sigma_{CL}/(T_{CL} - T_\infty) = 400 Gr_x^{-1/3} \tag{11}$$

$$\sigma_{CL}/(Q/\lambda Pr) = 4.00 \times 10^4 Gr_x^{-5/6} \tag{12}$$

The intensity[25] in the laminar region can be approximated by Eq. (14). From Eqs. (14) and (1), Eq. (13) is obtained and is shown by the solid line on the left side of Fig. 6a.

Laminar region:

$$\sigma_{CL}/(T_{CL} - T_\infty) = 10.0 \times 10^{-3} Gr_x^{1/6} \tag{13}$$

$$\sigma_{CL}/(Q/\lambda Pr) = 3.17 \times 10^{-3} Gr_x^{-1/30} \tag{14}$$

The data in the initial transitional region are approximated by Eq. (15) and are shown by the chain line. Equation (16) is obtained from Eqs. (15) and (3) as follows.

Initial transitional region:

$$\sigma_{CL}/(T_{CL} - T_\infty) = 3.17 \times 10^{-5} Gr^{7/15} \tag{15}$$

$$\sigma_{CL}/(Q/\lambda Pr) = 3.17 \times 10^{-3} Gr_x^{-1/30} \tag{16}$$

Although not shown in a figure, the intensity at a high rate agrees well with Eqs. (14), (16), (12), and (10) in the diagram[26] of $Q/\lambda Pr - Gr_x$. The intensity is proportional to $Q^m x^n$, where m and n are shown in Table 1. The intensity, i.e., the temperature amplitude in Fig. 3a, decreases rapidly in the final transitional and the turbulent regions because of turbulent diffusion.

At the low rate, the measured data are compared with Eqs. (13), (15), (11), and (9) in Fig. 6a. The intensity in the transitional and turbulent regions is larger than that at the high rate, and the intensity does not decrease in the turbulent region.

Given Height

Figure 6b shows the measured data of the intensity on the given height. The intensity[25] in the outer layer of the laminar plume[4] was between two solid lines. The intensity in the outer layer of the plume with transitional state at $y = 0$ is on the broken line with the same slope as the solid line. With increasing y, the intensity with turbulent state at $y = 0$ slightly increases, and then greatly decreases in the outer layer. Although not shown in a diagram[27] of $\sigma/(T_{CL} - T_\infty) - \xi$, the turbulent intensity is distributed on a single line at the high rate, but not at the low rate. This fact relates to the character of the time-averaged temperature at the given height, described earlier.

Grashof Number at Boundary Between Initial and Final Transitional Stages

As seen in Fig. 6a, the transitional region at the low and high rates is divided at Gr_b into two parts; one is the initial stage with poor generation of turbulence, and the other is the final stage with rather rich turbulence generation. The value of Gr_b was determined by Eqs. (16) and (12) as follows:

$$Gr_b = 7.52 \times 10^8 \tag{17}$$

Probability Density Function and Autocorrelation Coefficient

The PDF and ACC on the midplane are shown in Figs. 7 and 8, respectively. In the laminar and initial transitional regions, the PDF has the maximum value at high temperature because of the constantly maximum temperature resulting from the swaying motion, as seen in Fig. 3a. This feature disappears near the end of transition. With increasing x, the PDF width decreases, which corresponds to the results at the midplane of the fluctuation intensity. The PDF maximum increases greatly near the end of transition. The correlation decreases gradually in the initial and final transitional regions, and becomes very small in the turbulent region because to the irregularity of turbulence. The preceding features appear at any heat rate.

Power Spectrum Density and Discussion

As described in the previous section, a flow state could not be determined by only observing the temperature, fluctuation, PDF, and ACC. The PSD is therefore obtained, and is discussed to determine the flow state.

Midplane

The plume PSD on the midplane is shown in Fig. 9. The PSD slopes are $-9/2$ and -8.0 at the small value of x, i.e., Gr_x. These slopes are equal with those in the laminar PSDs,[4] whose dominant frequency agrees well with the computed result.[5] The region with these slopes can therefore be regarded as laminar, whose PSD is caused only by the swaying motion and is shown by the white-colored circle and solid line, which is expressed as follows.

Laminar spectrum:

$$S(s) = 6.47 \times 10^{-7} Q(\mathrm{W\,m})^{3/2} f\,(\mathrm{Hz})^{-9/2} \tag{18}$$

$$S(s) = 1.00 \times 10^{-11} Q(\mathrm{W/m})^{8/3} f\,(\mathrm{Hz})^{-8.0} \tag{19}$$

The region with the same PSD slope $-5/3$ as that by the Kolmogorov's hypothesis,[28] is regarded as turbulent. The slopes were $-5/3$ and -3.0 at the large height. The turbulent PSD, therefore, always has the slopes of both $-5/3$ and -3.0 in the inertia-convective and inertia-diffusive subranges. These slopes occur also in the turbulent PSDs of the plume in a stably stratified ambient.[8] Turbulent PSDs are shown by the black-colored circle and solid line in Fig. 9, and are approximated at any heat rates as follows.

Turbulent spectrum:

$$S(s) = 0.130 f\,(\mathrm{Hz})^{-5/3} \tag{20}$$

$$S(s) = 0.275 f\,(\mathrm{Hz})^{-3.0} \tag{21}$$

The region between the laminar and turbulent PSDs can be regarded as transitional, whose PSD is shown by the half white-colored circle. With increasing height, the PSD changes gradually in the initial transitional region, and rapidly approaches the turbulent PSD in the final region because of the rather rich generation of turbulence.

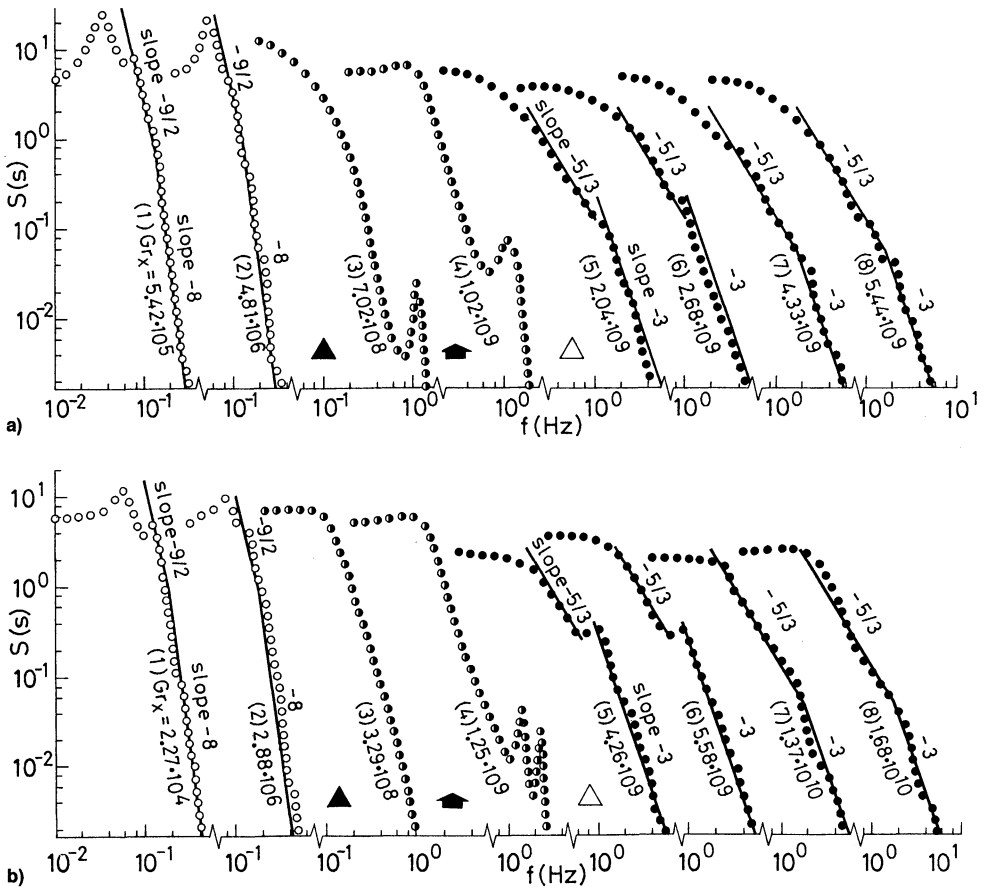

Fig. 9 PSD on midplane. At Q = a) 27.8 and b) 83.6 W/m.

Criterion for Determining Laminar, Transitional, and Turbulent Regions

A criterion for determining laminar, transitional, and turbulent states is as follows. Laminar PSDs are approximated by Eqs. (18) and (19), with slopes $-9/2$ and -8.0, and turbulent PSDs by Eqs. (20) and (21), with gradients of $-5/3$ and -3.0. Transitional PSDs are between the laminar and turbulent PSDs.

Critical Grashof Numbers

The laminar, transitional, and turbulent regions on the midplane were determined by the present criterion. From Fig. 9, and much other data, the approximate parameter to indicate transition is the following critical Grashof numbers Gr_s and Gr_e for the beginning and end of transition on the midplane, and the downstream distance x is not an additional parameter:

$$Gr_s = 2.0 \times 10^8 \tag{22}$$

$$Gr_e = 2.0 \times 10^9 \tag{23}$$

Forstrom and Sparrow[1] obtained Grashof numbers at $1.77 \leqq Q$ W/m $\leqq 17.1$ as follows:

$$Gr_s = 5.0 \times 10^8, \qquad Gr_e = 5.0 \times 10^9$$

Bill and Gebhart[12] obtained Grashof numbers at $13.0 \leqq Q$ W/m $\leqq 67.8$ as follows:

$$Gr_s = 1.12 \times 10^9, \qquad Gr_e = 7.9 \times 10^9$$

Critical Grashof numbers in the previous study[1,12] are slightly larger than those in the present study, as seen in Fig. 4a. This difference is caused by the different methods of determination. The first signs[1,12] of turbulent bursts or local turbulence for the beginning of transition depend on the time constant of a thermocouple. The visual determination[1,12] of a thickening of the plume for the end of transition has a difference among individuals.

Given Height

The PSD on the given height with turbulent and final transitional states at $y = 0$ is shown in Fig. 10, where the solid lines show the distributions of Eqs. (18–21). In Fig. 10a, even though apart from the midplane, the PSD in $0 \leqq \xi \leqq 7.0$ is approximated by Eqs. (20) and (21). The turbulent PSD therefore can be certainly expressed by Eqs. (20) and (21) at any location, i.e., on the midplane and the given height, and is independent of Q, which indicates that turbulence is governed by local conditions. The PSDs in Fig. 10b differ from the turbulent PSD, approaching solid lines of Eqs. (18) and (19) near $\xi = 20.0$, and are therefore in the transitional region. In Fig. 10c, the PSD is between the turbulent PSD and Eqs. (18) and (19), and approaches Eqs. (18) and (19) near $\xi = 14.0$. The PSD of laminar state in the turbulent plume on the given height is therefore approximated by Eqs. (18) and (19). This indicates that the intermittent entrainment in the outer layer of the turbulent plume is controlled by the swaying motion.

Thus, the turbulent state on the midplane changes to a transitional one and approaches a laminar state with an increase of y on the given height. This fact can be elucidated by employing the present criterion, but cannot be found by the existing methods.[1,12]

Frequency

With increasing ξ on the given height, the dominant frequency determined by the PSD decreases in the laminar region but does not vary in the turbulent region. The dominant frequency in laminar PSD apart from $\xi = 0$ is equal to the swaying frequency. The dominant frequency in turbulent PSD is

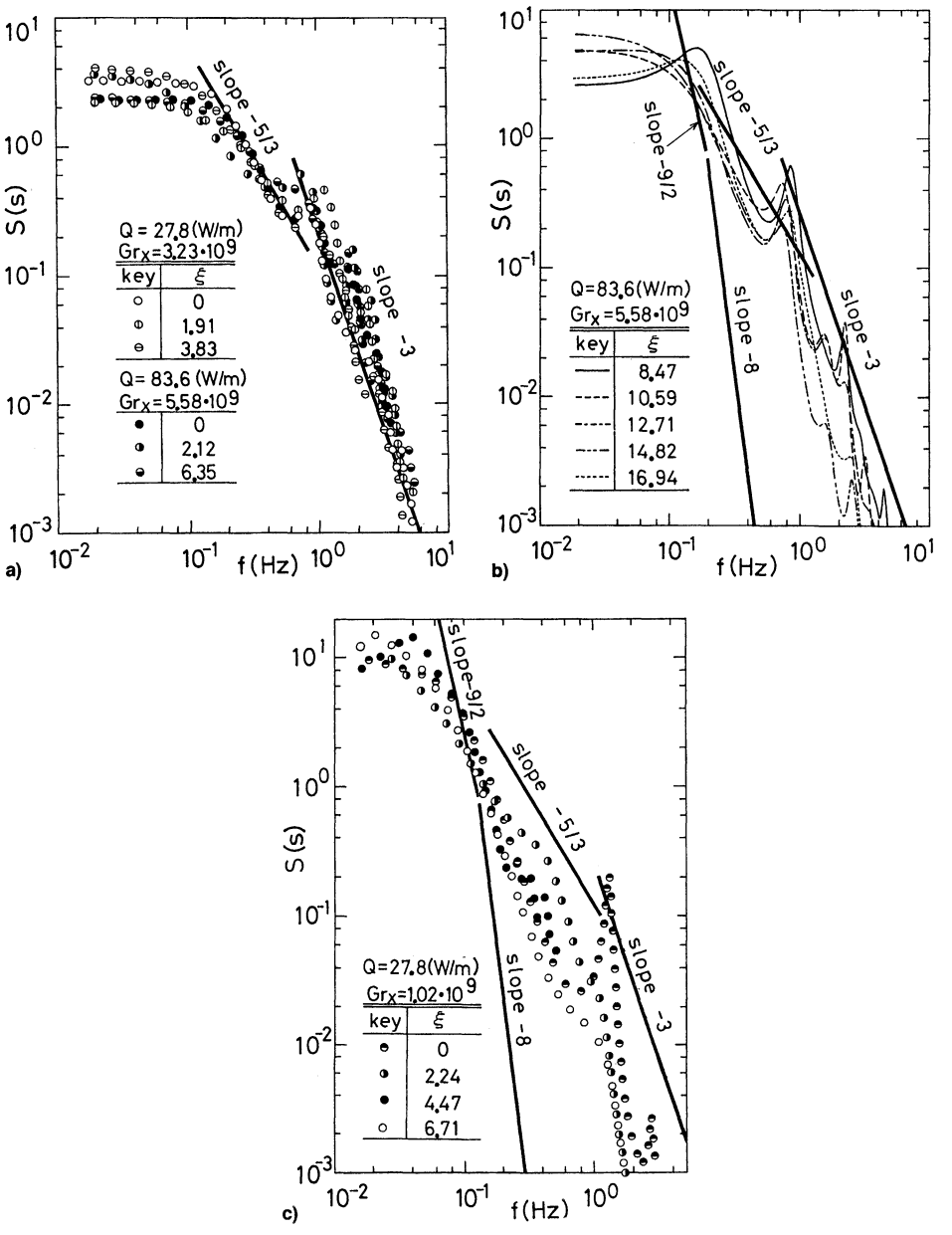

Fig. 10 PSD on given height. Turbulent at midplane at a) turbulent region at Q = 27.8 and 83.6 W/m, b) transitional region at Q = 83.6 W/m, and c) transitional at midplane and Q = 27.8 W/m.

equal to frequencies of the large vortices and the swaying motion. Thus, the turbulent PSD is certainly a result of both turbulence and swaying motion. The frequency band of turbulence differs from that of the swaying motion. That is, the frequencies of the turbulent PSD are much higher than those of the laminar PSD in Fig. 10b, and the swaying frequency is lower than that of turbulence. In PSD diagrams, it is possible to distinguish the swaying motion from turbulence. Bill and Gebhart[12] showed that the frequency range broadens gradually from the laminar to transitional region, and this agrees with the present result.

Advantage of Present Criterion

Thus, the existing methods[1,12] are based on qualitative determination and can be applied only on the midplane. However, the present method based on quantitative determination defined by Eqs. (18–21) is more precise and reasonable than those in the existing methods[1,12] and, therefore, is applicable to any location in any type of thermal flow. Regions of turbulent transition, reverse transition, and relaminarization occurring on not only the midplane but also other locations in the plume[8] in a stably stratified ambient can be determined by the present method, but cannot be determined by the existing methods.[1,12]

Conclusions

Spectra, regions of flow states, transition limits, the appropriate parameter for it, and turbulent transition characteristics of the thermal plume above a horizontal line heat source in unstratified air are revealed as follows:

1) Large-scale vortices occur in the turbulent region and have the same frequency as the laminar swaying motion, because the dominant frequency in turbulent PSD is equal to frequencies of the large vortices and the swaying motion.

2) Turbulent PSDs on the midplane and the given height have slopes of −5/3 and −3.0 in the inertia-convective and inertia-diffusive subranges.

3) A criterion for exactly determining a flow regime, i.e., laminar, transitional, and turbulent, at any location, i.e., on both the midplane and the given height, and at any heat rate is established as follows:

The laminar regime has the PSDs of $S(s) = 6.47 \times 10^{-7} Q(\mathrm{W/m})^{3/2} f(\mathrm{Hz})^{-9/2}$ and $S(s) = 1.00 \times 10^{-11} Q(\mathrm{W/m})^{8/3} (\mathrm{Hz})^{-8.0}$.

The turbulent regime has the PSDs of $S(s) = 0.130 f(\mathrm{Hz})^{-5/3}$ and $S(s) = 0.275 f(\mathrm{Hz})^{-3.0}$.

The transitional regime has the PSD between laminar and turbulent.

4) The appropriate parameter to indicate transition is the Grashof number, and the downstream distance x is not an additional parameter.

5) Critical Grashof numbers determined by spectra for the beginning and end of transition on the midplane are $Gr_s = 2.0 \times 10^8$ and $Gr_e = 2.0 \times 10^9$. The preceding Grashof numbers are slightly smaller than those in existing results[1,12] because of the differences of determining methods.

6) The transitional region is divided at the Grashof number Gr_b (=7.52×10^8) into the initial stage with the poor generation of turbulence and the final stage with the rich generation of turbulence.

7) The laminar and turbulent half-widths at the high rate are

$$\delta/(\lambda \nu^2 Pr/g\beta Q)^{1/3} = 2.50 Gr_x^{2/15}$$

$$\delta/(\lambda \nu^2 Pr/g\beta Q)^{1/3} = 18.0 Gr_x^{2/15}$$

The half-width at the end of transition is 9.8 times as thick as that at the beginning of transition.

8) The time-averaged temperatures on the midplane in the transitional and turbulent regions are expressed, respectively, by $(T_{CL} - T_\infty)/[Qh(0)/\lambda Pr] = 2.67 \times 10^2 Gr_x^{-1/2}$ and $(T_{CL} - T_\infty)/[Qh(0)/\lambda Pr] = 7.52 Gr_x^{-1/3}$.

9) The time-averaged and time-dependent properties of the plume are well interpreted by employing flow regions.

References

[1]Forstrom, R. J., and Sparrow, E. M., "Experiments on the Buoyant Plume Above a Heated Horizontal Wire," *International Journal of Heat and Mass Transfer*, Vol. 10, 1967, pp. 321–331.

[2]Schorr, A. W., and Gebhart, B., "An Experimental Investigation of Natural Convection Wakes Above a Line Heat Source," *International Journal of Heat and Mass Transfer*, Vol. 13, 1970, pp. 557–571.

[3]Fujii, T., Morioka, I., and Uehara, H., "Buoyant Plume Above a Horizontal Line Heat Source," *International Journal of Heat and Mass Transfer*, Vol. 16, 1973, pp. 755–768.

[4]Noto, K., "Swaying Motion in Thermal Plume Above a Horizontal Line Heat Source," *Journal of Thermophysics and Heat Transfer*, Vol. 3, 1989, pp. 428–434.

[5]Desrayaud, G., and Lauriat, G., "Unsteady Confined Buoyant Plumes," *Journal of Fluid Mechanics*, Vol. 252, 1993, pp. 617–646.

[6]Noto, K., Matsui, S., and Matsumoto, R., "Observation on Vortex Pair of Plane Thermal Plume in Thermally Stratified Fluid," *Flow Visualization IV*, edited by C. Veret, Springer–Verlag, Berlin, 1982, pp. 697–702.

[7]Noto, K., Honda, M., and Matsumoto, R., "Coherent Motion of Turbulent Thermal Plume in Stably Stratified Fluid," *Fluid Dynamics Research*, Vol. 3, 1988, pp. 415–421.

[8]Noto, K., Meguro, Y., and Nakajima, T., "Turbulent Enhancement, Reverse Transition, and Relaminarization in the Plume with Amplified Swaying Motion Due to Stably Stratified Ambient," *Proceedings of the 10th Symposium on Turbulent Shear Flows*, Vol. 3, 1995, pp. 61–66.

[9]Noto, K., "Dependence of Heat Island Phenomena on Stable Stratification and Heat Quantity in a Calm Environment," *International Journal of the Atmospheric Environment*, Vol. 30, No. 3, 1996, pp. 475–485.

[10]Rouse, H., Yih, C., and Humphreys, H., "Gravitational Convection from a Boundary Source," *Tellus*, Vol. 4, 1952, pp. 201–210.

[11]Lee, S. L., and Emmons, H. W., "A Study of Natural Convection Above a Line Fire," *Journal of Fluid Mechanics*, Vol. 11, 1961, pp. 353–368.

[12]Bill, R. G., and Gebhart, B., "The Transition of Plane Plumes," *International Journal of Heat and Mass Transfer*, Vol. 18, 1975, pp. 513–526.

[13]Gebhart, B., and Mahajan, R. L., "Instability and Transition in Buoyancy-Induced Flows," *Advance in Applied Mechanics*, Vol. 22, 1982, pp. 231–315.

[14]Gebhart, B., et al., *Buoyancy-Induced Flows and Transport*, Springer–Verlag, 1988, pp. 547–655.

[15]Mahajan, R. L., and Gebhart, B., "An Experimental Determination of Transition Limits in a vertical Natural Convection Flow Adjacent to a Surface," *Journal of Fluid Mechanics*, Vol. 91, 1979, pp. 131–154.

[16]Kotsovinos, N., and List, E. J., "Plume Turbulent Buoyant Jets (Part 1. Integral Properties)," *Journal of Fluid Mechanics*, Vol. 81, 1977, pp. 25–44.

[17]Ramapran, B. R., and Chandrasekhara, M. S., "Measurements in Vertical Plane Turbulent Plumes," *Journal of Fluid Engineering*, Vol. 111, 1989, pp. 69–77.

[18]Noto, K., and Matsumoto, R., "Swaying Motion in Thermal Plume Above a Line Heat Source (Spectrum Analysis of Swaying Wave by Means of the MEM)," *Memoirs of Faculty of Engineering*, No. 31, Kobe Univ., Kobe, Japan, 1984, pp. 103–112.

[19]Ulrych, T. J., and Bishop, T. N., "Maximum Entropy Spectral Analysis and Autoregressive Decomposition," *Review of Geophysics and Space Physics*, Vol. 13, 1975, pp. 183–200.

[20]Hino, M., *Spectral Analyses*, Asakura, Tokyo, 1977 (in Japanese).

[21]Noto, K., Honda, M., and Nakajima, T., "Time-Averaged Temperature Characteristics in Transition and Turbulent Regions of the Plume Above a Line Heat Source," *Trans. JSME, Series B*, Vol. 59, 1993, pp. 513–520 (in Japanese).

[22]Brodowicz, K., and Kierkus, W. T., "Experimental Investigation of Laminar Free-Convection Flow in Air Above Horizontal Wire with Constant Heat Flux," *International Journal of Heat and Mass Transfer*, Vol. 9, 1966, pp. 81–94.

[23]Lyakhov, Y. N., "Experimental Investigation of Free Convection Above a Heated Horizontal Wire," *Journal of Applied Mechanics and Technical Physics*, Vol. 11, 1970, pp. 355–359.

[24]Fujii, T., "Theory of Steady Laminar Natural Convection Above a Horizontal Line Heat Source and a Point Source," *International Journal of Heat and Mass Transfer*, Vol. 6, 1963, pp. 597–606.

[25]Noto, K., Yamazaki, Y., Ishida, H., and Matsumoto, R., "Swaying Motion of the Buoyant Plume Above a Horizontal Line Heat Source," *Trans. JSME, Series B*, Vol. 50, 1984, pp. 2179–2188 (in Japanese).

[26]Noto, K., Teramoto, K., and Nakajima, T., "Turbulent Transition and the Critical Grashof Number of the Thermal Plume Above a Line Heat Source in Unstratified Air," *Proceedings of the 9th Symposium on Turbulent Shear Flows*, Vol. 2, 1993, pp. 1–6.

[27]Noto, K., Okamoto, H., and Nakajima, T., "Time-Dependent Temperature Characteristics in Transition and Turbulent Regions of the Plume Above a Line Heat Source," *Trans. JSME, Series B*, Vol. 59, 1993, pp. 521–528 (in Japanese).

[28]Hinze, J. O., *Turbulence*, McGraw–Hill, New York, 1975.